Scaling invariance for the escape of particles from a periodically corrugated waveguide

Edson D. Leonel[1], Diogo R. da Costa[1,2] and Carl P. Dettmann[3]

[1] *Departamento de Estatística, Matemática Aplicada e Computação - UNESP - Univ Estadual Paulista Av.24A, 1515 - CEP: 13506-900 - Rio Claro - SP - Brazil*
[2] *Instituto de Física, Univ São Paulo, Rua do Matão, Cidade Universitária - CEP: 05314-970 - São Paulo - SP - Brazil*
[3] *School of Mathematics, University of Bristol, Bristol BS8 1TW, United Kingdom*

Abstract

The escape dynamics of a classical light ray inside a corrugated waveguide is characterised by the use of scaling arguments. The model is described via a two dimensional nonlinear and area preserving mapping. The phase space of the mapping contains a set of periodic islands surrounded by a large chaotic sea that is confined by a set of invariant tori. When a hole is introduced in the chaotic sea, letting the ray escape, the histogram of frequency of the number of escaping particles exhibits rapid growth, reaching a maximum value at n_p and later decaying asymptotically to zero. The behaviour of the histogram of escape frequency is characterised using scaling arguments. The scaling formalism is widely applicable to critical phenomena and useful in characterisation of phase transitions, including transitions from limited to unlimited energy growth in two dimensional time varying billiard problems.

Key words: Corrugated waveguide, two dimensional mapping, transport properties
PACS: 05.45.-a, 05.45.Ac, 05.45.Pq

1 Introduction

Guiding a light ray inside a periodically corrugated waveguide has been of interest for many years. This subject appears in many different fields of science including transport through a finite $\mathrm{GaAs/Al_xGa_{1-x}As}$ hetero-structure (1), quantum transport in ballistic cavities (2), quantised ballistic conductance in a periodically modulated quantum channel (3), underwater acoustics (4; 5; 6), classical versus quantum behaviour in periodic mesoscopic systems (7), scattering of a quantum particle in a rippled waveguide (8), anomalous wave transmittance in the stop band of a corrugated parallel-plane waveguide (9) and many others (10; 11).

The formalism we use to describe the dynamics is the billiard approach [1] and the dynamics is described by the use of discrete maps. Depending on the geometry, the phase space for such maps is in one of three classes: (i) regular, (ii) ergodic and (iii) mixed. For the regular case, only periodic and quasi-periodic orbits are observed in the phase space. For the completely ergodic billiards the opposite happens: only chaotic and unstable orbits are present in the dynamics. The Bunimovich stadium (12) and the Sinai billiard (13) (and related Lorentz gas) are examples of case (ii). In this case the time evolution of a single typical initial condition, for the appropriate combinations of control parameters, fills up ergodically all the phase space. For the last case (iii), there are many systems presenting mixed phase space structure (14; 15; 16; 17; 18). Depending on the combinations of both initial conditions and control parameters, the phase space presents a rich structure which contains invariant spanning curves, periodic islands and chaotic seas. The mixed structure leads to sticky regions (19) and therefore to non-uniformity (20) producing anomalous transport. It is well known that a sticky region keeps a particle trapped in the phase space and the escape from such a region happens after long time late the entrance.

This stickiness can be characterised in terms of the distribution of recurrence times. Similarly, statistics may be considered for the time taken to reach a given region (the "hole(s)") from initial phase points distributed (for example uniformly) throughout the system (an escape problem), or entering from one region and exiting through another (classical scattering). These problems have been considered for several decades (21; 22); more recent discussion and references, with particular reference to theory and applications of billiards, may be found in (23). For mixed phase space, all these distributions typically exhibit a power law decay (24) while they are exponential for fully developed chaos (25); some exceptions have been noted very recently (26; 27).

In this paper, we revisit the problem of a periodic corrugated waveguide seeking to understand and describe some statistical properties of dynamics in the chaotic sea, in particular the escape of particles from a hole we place in the chaotic region. The histogram of frequency of escape shows a fast regime of growth for short time and passes a maximum value. After that it decreases approaching zero for long times. The maximum value was used to characterise the scaling invariance of the histogram of frequency of escape.

The model consists of a classical light ray which is specularly reflected [2] be-

[1] A billiard problem consists of a system in which a point-like particle moves freely inside a bounded region and suffers specular reflections with the boundaries.
[2] In a specular reflection the angle of incidence is equal to the angle of reflection.

tween a flat plane at $y = 0$ and a corrugated surface given by $y = y_0 + d\cos(kx)$, where y_0 is the average vertical distance between the flat plane and the corrugated surface, d is the amplitude of the corrugation and k is the wave number. The dynamical variables used in the study are the angle θ of the trajectory measured from the positive horizontal axis and the corresponding value of the coordinate x at the instant of the reflection. The mapping is iterated when the ray light *hits* the flat plane. It implies that multiple reflections with the periodically corrugated surface are neglected[3] (28). An estimation of the position of the two first invariant spanning curves (positive and negative) delimiting the size of the chaotic sea is given in terms of a connection with the Standard map. Also, the behaviour of the positive Lyapunov exponent for a large range of control parameters is investigated.

This paper is organised as follows. In section 2, we present and discuss the details needed to construct the non linear mapping. We also discuss the procedures used to obtain the Lyapunov exponents. Some results for the phase space are also discussed in connection with the Standard map. In section 3 the scaling results for the escape of particles statistics are obtained and discussed. Finally, the conclusions and final remarks are given in section 4.

2 The model and the nonlinear mapping

In this section, we discuss all the details needed to describe the model and obtain the equations that give the dynamics of the system. The problem consists in obtaining a mapping $T(\theta_n, x_n) = (\theta_{n+1}, x_{n+1})$, given the initial conditions (θ_n, x_n) as shown in Fig. 1(a). The mapping is obtained only from geometrical considerations of Fig. 1(b). The first part of the light trajectory is given by

$$x_n^* - x_n = (y_0 + d\cos(kx_n^*))/\tan(\theta_n) \ .$$

and in a similar way, the second part is

$$x_{n+1} - x_n^* = (y_0 + d\cos(kx_n^*))/\tan(\theta_{n+1}) \ . \quad (1)$$

The term x_n^* gives the exact location of the collision on the corrugated surface. On the other hand, the angle θ_n is written as

$$\theta_{n+1} = \theta_n - 2\psi_n \ , \quad (2)$$

See details in Fig. 1(b).

[3] This is a standard approximation which is very useful to speed up the numerical simulations since no transcendental equations must be solved, as they have to be in the corresponding complete version of the problem.

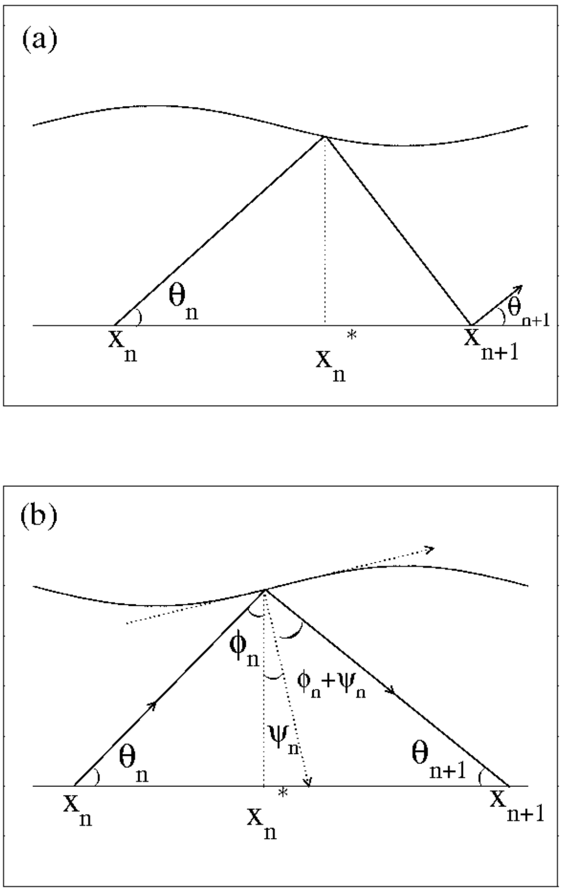

Fig. 1. (a) Reflection from the corrugated surface of a light ray coming from the flat surface at $y = 0$. (b) Details of the trajectory before and after a collision with the corrugated surface.

where $\tan(\psi_n(x)) = dy(x)/dx = -dk \sin(kx_n^*)$ gives the slope of the corrugated surface at the point $x = x_n^*$. The condition of specular reflection was used in the derivation of the Eq. (2). Equations (1) and (2) correspond to the exact form of the mapping. In this paper however, we consider only a simplified version. In this sense, the following approximations are taken into account:

(1) The relative corrugation is assumed to be small. It implies that $d/y_0 \ll 1$, yielding $y_0 + d\cos(kx_n^*) \cong y_0$;
(2) For the limit of small corrugation, it is also assumed that $\tan(\psi_n) \cong \psi_n$.
(3) Considering small reflection angles we have $\tan(\theta_n) \cong \theta_n$.

We note that the approximation of small relative corrugation is singular: For $d = 0$, the system is integrable, since the two boundaries are parallel plates and the phase space shows only straight lines. However, if $d \neq 0$ the phase space becomes mixed and exhibits chaos, invariant spanning curves and periodic islands. There is an abrupt transition from integrability to non integrability when the control parameter goes from $d = 0$ to $d \neq 0$.

Before writing the equations of the mapping, we note that there are an excessive number of control parameters, namely d, k, y_0. The dynamics does not depend on all of them. It is convenient to define the following dimensionless variables $\delta = d/y_0$, $\gamma_n = \theta_n/y_0k$ and finally $X_n = kx_n$. With this set of new variables, the only relevant control parameter is δ. The two dimensional non linear mapping is given by

$$T : \begin{cases} X_{n+1} = X_n + \left[\frac{1}{\gamma_n} + \frac{1}{\gamma_{n+1}}\right] \mod(2\pi) \\ \gamma_{n+1} = \gamma_n + 2\delta \sin\left(X_n + \frac{1}{\gamma_n}\right) \end{cases} . \quad (3)$$

The determinant of the Jacobian matrix is the unity and the mapping preserves the phase space area.

Figure 2 shows the phase space generated by the iteration of mapping (3). One sees that there is a complex structure containing periodic islands surrounded by a large chaotic sea that is confined between two invariant spanning curves, where one is positive and other negative. The chaotic sea was characterised using Lyapunov exponents. These shows great applicability as a practical tool that can quantify the average expansion or contraction rate for a small volume of initial conditions. As discussed in (29), the Lyapunov exponents are defined as

$$\lambda_j = \lim_{n\to\infty} \frac{1}{n} \ln|\Lambda_j| \quad , \quad j = 1, 2 \quad , \quad (4)$$

where Λ_j are the eigenvalues of $M = \prod_{i=1}^{n} J_i(\gamma_i, X_i)$ and J_i is the Jacobian matrix evaluated over the orbit (γ_i, X_i). If at least one of the λ_j is positive then the orbit is classified as chaotic. Therefore we define λ as the larger value of the λ_j. The average value for the positive Lyapunov exponent obtained for the control parameter $\delta = 10^{-3}$ was $\bar{\lambda} = 1.624(7)$ where the error 0.007 corresponds to the standard deviation of an ensemble of 10 different initial conditions chosen along the chaotic region. The behaviour of the positive Lyapunov exponent as a function of the control parameter δ is shown in Fig. 3. We see that the variation of the positive Lyapunov exponent is relatively small for the range of control parameters considered. For a range of three decades in the control parameter δ, namely $\delta \in [10^{-5}, 10^{-2}]$, the Lyapunov exponent varies by about 10%.

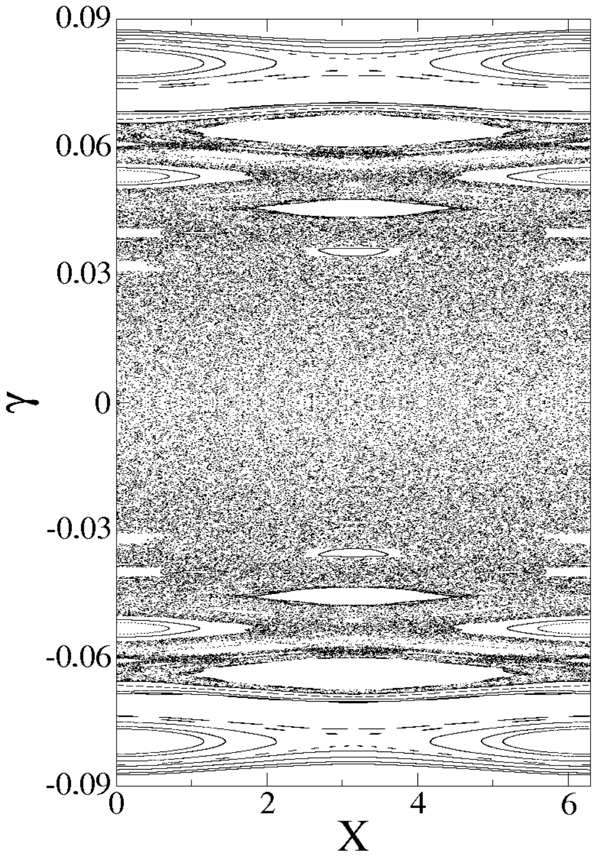

Fig. 2. Phase space for the mapping (3) with the control parameter $\delta = 10^{-3}$.

As the control parameter δ varies, consequently the edge of the chaotic sea and the position of the two first (positive and negative) invariant spanning curves vary too. Since these two curves separate global from local chaos, we expect that the dynamics of the system can be locally described using the Standard map. To do so, we follow similar procedure used in Ref. (30) and write the reflection angle as

$$\gamma_{n+1} \cong \gamma^* + \Delta\gamma_{n+1} \ , \tag{5}$$

where γ^* is a typical value of the reflection angle along the invariant spanning curve and $\Delta\gamma_{n+1}$ is a small perturbation of the angle. If we consider $Z_n = X_n + 1/\gamma_n$, rewrite the first equation of the mapping (3), expand it in Taylor series, rearrange the results and define the new variables $I_{n+1} = -\frac{2\Delta\gamma_{n+1}}{\gamma^{*2}} + \frac{2}{\gamma^*}$ and $\phi_n = Z_n + \pi$, we obtain the mapping

$$T : \begin{cases} I_{n+1} = I_n + \frac{4\delta}{\gamma^{*2}} \sin(\phi_n) \\ \phi_{n+1} = \phi_n + I_{n+1} \end{cases} \ , \tag{6}$$

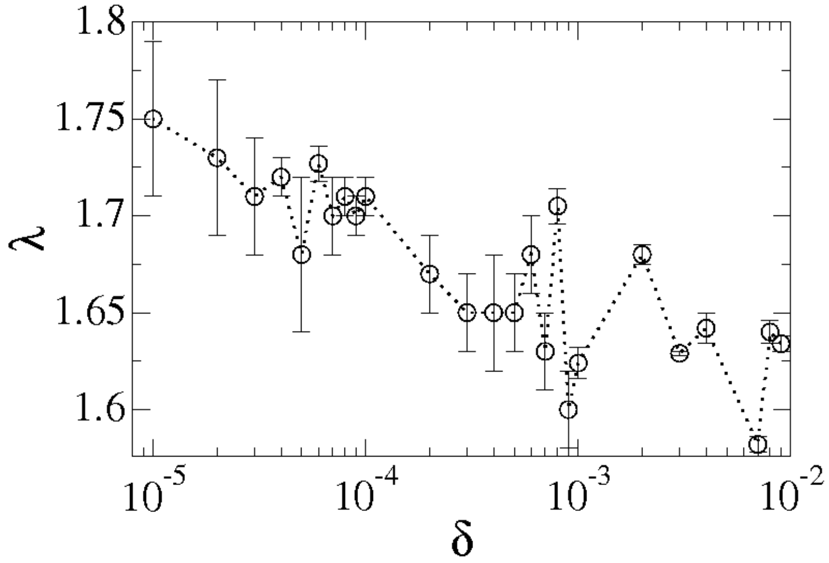

Fig. 3. The positive Lyapunov exponent as a function of the control parameter δ.

where one recognises an effective control parameter given by $K_{\mathrm{eff}} = 4\delta/\gamma^{*2}$. As discussed in Ref. (31), the transition from local to global chaos occurs at $K_{\mathrm{eff}} \cong 0.971\ldots$, we obtain that the two invariant spanning curves that limit the chaotic sea are given by

$$\gamma^* \cong \pm 2\sqrt{\frac{\delta}{0.971\ldots}}\ . \tag{7}$$

Therefore we can conclude that the *size* of the chaotic sea is proportional to $\sqrt{\delta}$ as previously discussed in Ref. (30). A numerical simulation was made in support of this result, as shown in Fig. 4

3 Scaling and escape of particles for the chaotic sea

In this section we introduce a hole in the chaotic sea letting the particle escape when reaching $|\gamma| \geq \gamma_c > 0$, where γ_c is always smaller than those observed in the first invariant spanning curve. Our main goal with this approach is to understand the dynamics of the escape, along the chaotic component of the dynamics, considering an ensemble of initial conditions. We give an initial condition along the chaotic sea with small initial $\gamma_0 = 10^{-5}\delta$ and a random X_0 and let the dynamics evolve for up to 10^7 collisions using an ensemble of 10^9 different initial conditions $X_0 \in [0, 2\pi)$. During the dynamics, if $|\gamma_n| \geq \gamma_c$, we interrupt the evolution, collect the number of collisions until that time and start a new initial condition. Using this procedure, we obtain a histogram of escape frequency, as shown in Fig. 5(a) for different control parameters as well

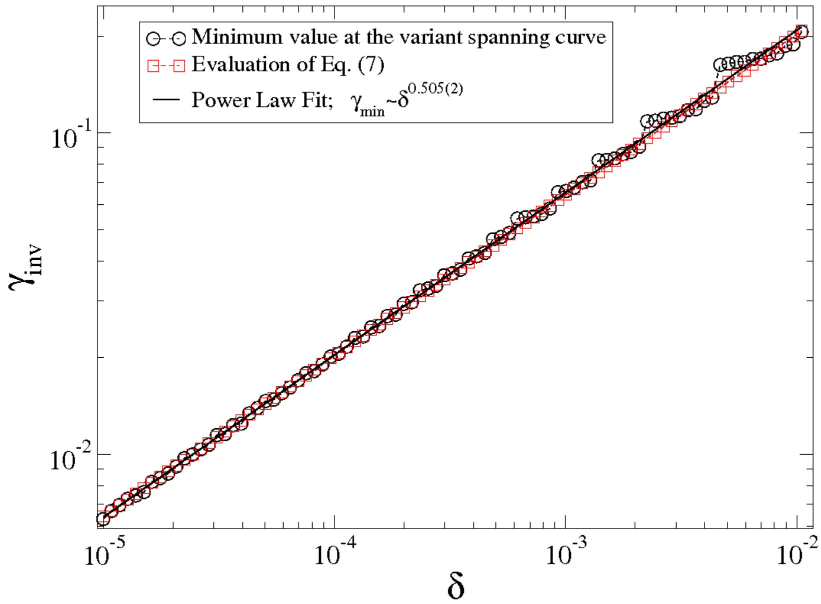

Fig. 4. Plot of the minimum value of γ at the first invariant spanning curve as a function of δ together with the evaluation of Eq. (7). A power law fitting gives $\gamma \propto \delta^{0.505(2)}$.

as different positions of the hole γ_c. We see a rapid growth for short n when the histogram reaches a maximum at n_p. After that there is a decay for large n approaching zero asymptotically. For the ensemble used, few orbits do not escape until 10^7. However the histogram shown in Fig. 5(a) was rescaled to maximum 10^5 only for visualisation. The peak position n_p is an increasing function of γ_c. A plot of n_p vs γ_c produces a power law with an exponent $u = 1.97(1)$ as shown in Fig. 6(a). If we consider the transport in this system as a normal Brownian diffusion, we would expect that n_p is proportional to γ_c^2. However, due to stickiness and trapping of particle near the islands, the exponent obtained is slightly smaller than 2, specifically 1.97(1), as shown in Fig. 6(a). A plot of n_p vs δ for different values of γ_c is shown in Fig. 6(b) for the following escape parameter, together with their power law fits: $\gamma_c = 20\%\gamma_{inv}$ with $\zeta = -0.950(8)$; $\gamma_c = 40\%\gamma_{inv}$ and $\zeta = -0.951(6)$; finally $\gamma_c = 70\%\gamma_{inv}$ with $\zeta = -0.97(2)$. The average $\bar{\zeta} = -0.95(1)$. Given now that the exponent $\bar{\zeta}$ is obtained, the histogram of escape frequency considered both as a function of δ and γ_c can be rescaled to overlap all curves onto a single plot as shown in Fig. 5(b).

This scaling invariance of the histogram of escape frequency was also observed for the problem of a particle confined inside an infinite box of potential containing a time varying well (32). The dynamics of that model was described by the use of a two dimensional nonlinear and area preserving mapping. The system has three relevant control parameters namely: (1) δ, controlling the relative amplitude of oscillation of the oscillating well; (2) N_c, controlling the

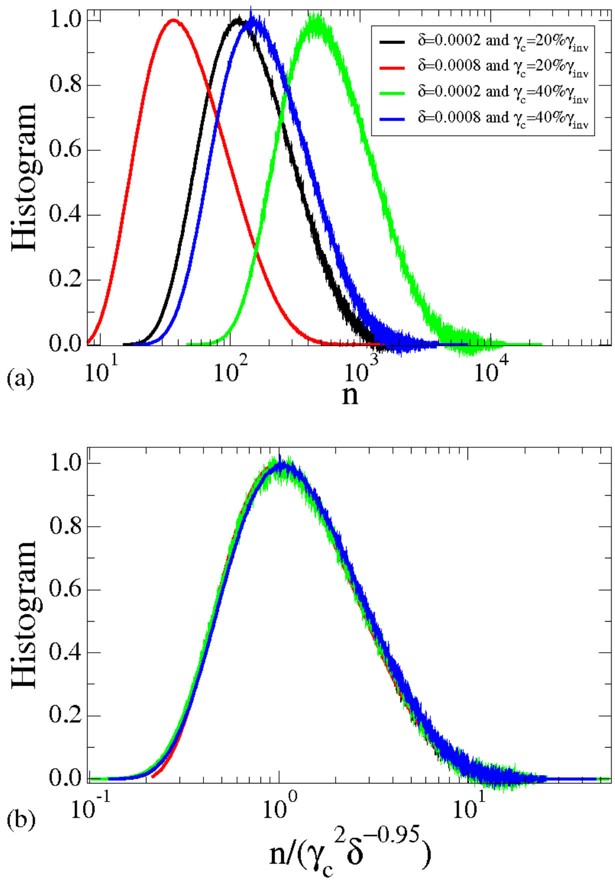

Fig. 5. (a) Histogram of escape frequency for different γ_c and different δ. (b) Overlap of all curves shown in (a) onto a single and universal plot after a rescale $n \rightarrow n(/\delta^{\bar{\zeta}}\gamma_c^u)$.

frequency of oscillation of the well and (3) r, controlling the relative width of the well with respect to the box of infinity potential. Each one of them leads to different exponents characterising the behaviour for n_p and scaling invariance for the behaviour of histogram of escape frequency is also observed. Despite the mixed structure of the phase space observed for both models, the exponent obtained for the peak of the histogram of escape is different for either models which must therefore arise from different average properties of the chaotic sea.

4 Summary and Conclusions

In summary, we have considered the problem of light ray reflection in a periodically corrugated waveguide. The chaotic sea confined between the first two (positive and negative) invariant spanning curves was characterised using scaling arguments together with a connection with the Standard map. When hole is introduced in the chaotic sea, the histogram of escape frequency exhibits a

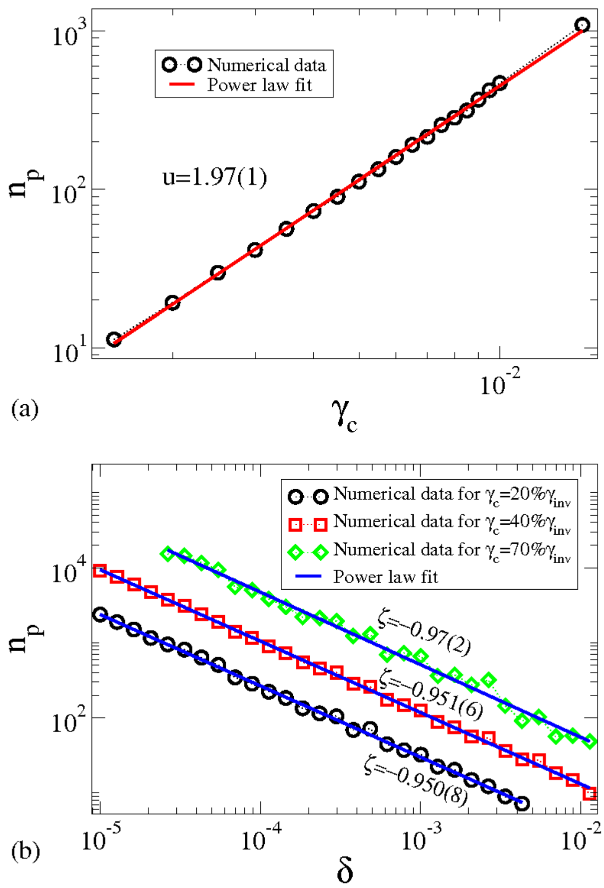

Fig. 6. (a) Plot of $n_p$vsγ_c. A power law fitting furnishes an exponent $u = 1.97(1)$. (b) Plot of $n_p \times \delta$ and respective power law fittings for $\gamma_c = 20\%\gamma_{inv}$ with $\zeta = -0.950(8)$; $\gamma_c = 40\%\gamma_{inv}$ with $\zeta = -0.951(6)$; and finally $\gamma_c = 70\%\gamma_{inv}$ with $\zeta = -0.97(2)$.

growth marked by a maximum and a decay at longer iterations (reflections). The maximum of the histogram was used to obtain scaling relations and to overlap all curves of the histogram obtained as function of the control parameter as well as the position of the escape, onto a single and universal plot. It would be interesting in the future to trace the signature of these scalings in the quantum regime.

Acknowledgments

E. D. L. thanks financial support from CNPq, FAPESP and FUNDUNESP, Brazilian agencies. D. R. C. thanks to CNPq. C. P. D is grateful to CNPq and PROPG-UNESP for his visit to DEMAC-UNESP/Rio Claro.

References

[1] Kouwenhoven L P, Hekking F W J , van Wees B J, Harmans C J P M, Timmering C E and Foxon C T. Transport through a finite one-dimensional crystal. Phys. Rev. Lett. 1990; 65: 361.

[2] Huckestein B, Ketzmerick R and Lewenkopf C H. Quantum transport through ballistic cavities: Soft vs hard quantum chaos. Phys. Rev. Lett. 2000; 84: 5504.

[3] Leng M and Lent C S. Recovery of quantized ballistic conductance in a periodically modulated channel. Phys. Rev. Lett. 1993; 71: 137.

[4] Virovlyansky A L and Zaslavsky G M. Evaluation of the smoothed interference pattern under conditions of ray chaos. Chaos 2000; 10: 211.

[5] Smirnov I P, Virovlyansky A L and Zaslavsky G M. Theory and applications of ray chaos to underwater acoustics. Phys. Rev. E 2001; 64: 036221.

[6] Iomin A and Bliokh Yu. Wave localization as a manifestation of ray chaos in underwater acoustics. Commun. Nonlinear. Sci. Numer. Simul. 2003; 8: 389.

[7] Luna-Acosta G A, Méndez-Bermúdez J A and Izrailev F M. Periodic chaotic billiards: Quantum-classical correspondence in energy space. Phys. Rev. E 2001; 64: 036206; Quantum-classical correspondence for local density of states and eigenfunctions of a chaotic periodic billiard. Phys. Lett. A 2000; 274: 192.

[8] Akguc G B and Reichl L E. Direct scattering processes and signatures of chaos in quantum waveguides. Phys. Rev. E 2003; 67: 046202.

[9] Hwang R B. Negative group velocity and anomalous transmission in a one-dimensionally periodic waveguide. IEEE Tran. Ant. and Prop. 2006; 54: 755.

[10] York A G, Milchberg H M, Palastro J P and Antonsen T M. Direct acceleration of electrons in a corrugated plasma waveguide. Phys. Rev. Lett 2008; 100: 195001.

[11] Craster R V, Guenneau S and Adams S D M. Mechanism for slow waves near cuttof frequencies in periodic waveguides. Phys. Rev. B 2009; 79: 045129.

[12] Bunimovich L A. Ergodic properties of nowhere dispersing billiards. Commun. Math. Phys. 1979; 65: 295.

[13] Sinai Y G. Dynamical systems with elastic reflections. Russian Math. Surveys 1970; 25: 137.

[14] Berry M V. Regularity and chaos in classical mechanics, illustrated by three deformations of a circular 'billiard'. Eur. J. Phys. 1981; 2: 91.

[15] Kamphorst S O and Carvalho S P. Bounded gain of energy on the breathing circle billiard. Nonlinearity 1999; 12: 1363.

[16] Robnik M. Classical dynamics of a family of billiards with analytic boundaries. J. Phys. A: Math. Gen. 1983; 16: 3971.

[17] Robnik M and Berry M V. Classical billiards in magnetic-fields. J. Phys. A: Math. Gen. 1985; 18: 1361.

[18] Markarian R, Kamphorst S O and de Carvalho S P. Chaotic properties of the elliptical stadium. Commun. Math. Phys. 1996; 174: 661.

[19] Zaslavsky G M. Physics of Chaos in Hamiltonian Systems (Imperial College Press; London 1998).

[20] Zaslavsky G M. Chaos, fractional kinetics, and anomalous transport. Phys. Rep. 2002; 371; 461.

[21] Lax P D, Phillips R S Scattering theory. Bull Amer Math Soc 1964; 70; 130.

[22] Pianigiani G, Yorke J A, Expanding maps on sets which are almost invariant: Decay and chaos Trans. Amer. Math. Soc. 1979; 252; 351.

[23] Dettmann C, Recent advances in billiards with some open problems, in Frontiers in the study of chaotic dynamical systems with open problems, Ed Zeraoulia E and Sprott J C 2011.

[24] Altmann E G, Motter A E, Kantz H. Stickiness in Hamiltonian systems: From sharply divided to hierarchical phase space. Phys. Rev. E 2006; 73; 026207.

[25] Altmann E G, da Silva E C, Caldas I L. Recurrence time statistics for finite size intervals. Chaos 2004; 14; 975.

[26] Dettmann C P, Georgiou O, Transmission and reflection in the stadium billiard: Time-dependent asymmetric transport, Phys. Rev. E 2011; 83; 036212.

[27] Dettmann C P, Leonel E D, Asymmetric transport in the bouncer model: mixed, time dependent, noncompact dynamics, arXiv:1010.2228

[28] Leonel E D. Corrugated waveguide under scaling investigation. Phys. Rev. Lett. 2007; 98: 114102.

[29] Eckmann J -P and Ruelle D. Ergodic-theory of chaos and strange attractors. Rev. Mod. Phys. 1985; 57: 617.

[30] Rabelo A F, Leonel E D. Finding Invariant Tori in the Problem of a Periodically Corrugated Waveguide. Brazilian Journal of Physics. 2008; 38: 54.

[31] Lichtenberg A J and Lieberman M A. Regular and Chaotic Dynamics (Appl. Math. Sci. **38**; Springer Verlag; New York 1992)

[32] da Costa D R, Dettmann D P, Leonel E D. Escape of particles in a time dependent potential well. Phys. Rev. E 2011; 83: 066211.